Cellulose nanocrystals: A layered host candidate for fabricating intercalated nanocomposites

Juan Guo [a,b], Wenbo Du [c], Siqun Wang [a,d], Yafang Yin [a,b,*], Yong Gao [c,**]

[a] Department of Wood Anatomy and Utilization, Research Institute of Wood Industry, Chinese Academy of Forestry, Beijing 100091, China
[b] Research Institute for Forestry New Technology, Chinese Academy of Forestry, Beijing 100091, China
[c] College of Chemistry, Xiangtan University, Xiangtan 411105, China
[d] Center for Renewable Carbon, University of Tennessee, Knoxville, TN 37996, USA

ARTICLE INFO

ABSTRACT

The stacking of cellulose chains along planes and weak intersheet interactions make cellulose nanocrystals (CNCs) promising as a layered host candidate for fabricating intercalated nanocomposites. As a proof-of-concept, we demonstrate the intercalation of alkyls into CNCs through the in situ intercalative chemical reaction between terminal groups of N-octadecyl isocyanates and hydroxyl groups on the (200) planes in CNCs. Results showed that CNCs could intercalate alkyls in a high degree of substitution to form dense brushes on their (200) planes. After intercalation, a significant enlargement of interlayer spacing was observed. Moreover, alkyls were fully extended in all-trans configuration and crystallized in a co-existing organization of α_H, β_H and β_O crystalline forms. This meant that the molecular arrangement in CNCs/alkyl intercalated nanocomposites would involve a bilayer model in which alkyls were in the ordered packing and tilted to (200) plane. Furthermore, CNCs/alkyl intercalated nanocomposites possessed increased thermal properties and decreased char residue.

© 2016 Elsevier Ltd. All rights reserved.

1. Introduction

Fabrication of intercalated structure, in which guest molecules or ions are intercalated into a layered host solid without the major rearrangement of host structure (Whittingham, 1982), is a significant method to develop ordered hierarchical systems. Until now, amounts of advanced intercalated nanocomposites possessing decreased gas permeability and flammability, increased thermal properties, unique optical properties and heterogeneous catalytic properties have been fabricated (Deng et al., 2012; Guo, Zhu, Jiang, & Chen, 2011; Ray & Okamoto, 2003; Roth, Gil, Makowski, Marszalek, & Eliášová, 2016).

Among the potential layered hosts for fabricating intercalated nanocomposites, inorganic materials such as silicate, graphite, metal oxides and layered double hydroxides have been widely reported (Oshima, Lu, Ishitani, & Maeda, 2015; Ray & Okamoto, 2003; Zhang, Hou et al., 2016). In contrast, only a limited number

of organic materials has been successfully used to fabricate intercalated nanocomposites, such as sodium calix[4]arenesulfonate compolexes (Bott, Coleman, & Atwood, 1988), cholic acid (Miyata et al., 1990), organic laminates (Biradha, Dennis, MacKinnon, Sharma, & Zaworotko, 1998), and polymer crystals (Giovanella et al., 2014; Matsumoto, Odani, Sada, Miyata, & Tashiro, 2000). This is due to the difficulty of maintaining the layered structure during intercalation when an organic sheet consists of noncovalent bonds between the low-molecular-weight compounds, instead of covalent bonds in an inorganic sheet (Oshita & Matsumoto, 2006). In biology, a variety of organisms do exert control over the intercalation of some macromolecules into the crystal lattice (Berman et al., 1993). While, till now, very few examples of intercalation system using bioorganic materials as the host have been reported (Rädler, Koltover, Salditt, & Safinya, 1997). Considering the attractive features of bioorganic materials such as commonly available, renewable, sustainable, facile functionality and low environmental, animal/human health and safety risks, developments of intercalated nanocomposites using bioorganic materials as the host should further extent the application of intercalated materials.

Cellulose nanocrystals (CNCs) are natural cellulose based nanomaterials, which are isolated from cellulose raw materials easily and efficiently (Habibi, Luci, & Rojas, 2010; Lu et al., 2016; Zhang, Sun et al., 2016). As a new bioorganic material, CNCs exhibit amaz-

---

ing properties, including high crystallinity, exceptional mechanical properties, a larger specific surface area, a high aspect ratio, amazing liquid crystal properties and environmental benefits (Ma, Zhang, Meng, & Wang, 2015; Majoinen et al., 2016; Wang, Hamad, & MacLachlan, 2016). Besides, CNCs have the highly orientated crystallite structure due to the cellulose microfibril biosynthesis (Moon, Martin, Nairn, Simonsen, & Youngblood, 2011). Parallel stacking of cellulose chains in one plane is present along the $(200)_m$ and $(110)_t$ planes, which is also called "hydrogen-bonded planes". In the (200) planes of CNCs I_β (monoclinic structure) polymorph for instance, strong intrachain hydrogen bonding $O(3)H \cdots O(5)$ bond and intra- and inter-chain bonding $O(2)H \cdots O(6)$ and $O(6)H \cdots O(2)$ bonds are prevalent. And weaker intersheet interactions such as $CH \cdots O$ hydrogen bonding and van der Waals forces are responsible for the neighboring (200) planes (Moon et al., 2011). Therefore, delamination of (200) lattice planes has been reported when the intersheet interactions are partially dissociated (Guo, Guo et al., 2016; Li & Renneckar, 2011). Deriving from these structure properties similar to layered inorganic hosts, i.e. layered double hydroxides, as well as the nanosized morphology, abundant reactive hydroxyl groups and the relative high melting point, CNCs have the potential as a layered host candidate for fabricating intercalated nanocomposites. It is therefore deemed necessary to investigate the structure variations of CNCs after an in situ intercalative chemical reaction and to clarify their ability as the intercalated host.

In this paper, CNCs isolated from filter papers by sulfuric acid hydrolysis during ultrasonic treatment and n-octadecyl isocyanate were used as the intercalation host and the intercalation guest, respectively for the fabrication of CNCs/alkyl intercalated nanocomposites. N-octadecyl isocyanate was intercalated into CNCs through the in situ intercalative chemical reaction between n-octadecyl isocyanate molecules and hydroxyl groups on the (200) planes in CNCs. X-ray diffraction (XRD), Fourier transform infrared (FT-IR) spectroscopy and elemental analysis were used for illustrating the intercalation structure. And the crystallization of long chain alkyl in intercalated CNCs was investigated by Differential Scanning Calorimetry (DSC). In addition, Thermogravimetric Analysis (TGA) was used to investigate the thermal properties of CNCs after the intercalation. The present study would provide a scientific basis for the development of intercalated materials using CNCs and also further extent the application of CNCs in the intercalated nanocomposites field.

2. Experimental

2.1. Materials

Cellulose filters (softwood sulfite pulp) were purchased from the Xinhua Paper Mill (Hangzhou, China). N-octadecyl isocyanate and dibutyl dilauryl were purchased from Sigma-Aldrich (France). Sulfuric acid, ethanol and dichloromethane were purchased from the Beijing Chemical Reagent Company (Beijing, China) and were used without further purification. Toluene was dried and purified according to standard procedures. Dialysis bags (Mw cut off 14,000) were purchased from the Greenbird Company (Shanghai, China).

2.2. Preparation of cellulose nanocrystals

CNCs were prepared by acid hydrolysis during ultrasonic treatment followed our previous study (Guo, Guo et al., 2016). 15 g of cellulose was immersed in 150 mL of sulfuric acid solution (64 wt%) in a round flask. The hydrolysis was carried out at 45 °C for 120 min in an ultrasonic cleaner, at a frequency of 40 kHz, a power density of 0.48 Wcm^{-2} and a power output of 405 W (DL-480B, Shanghai Zhixin Instrument Co. Ltd, China). Following this, deionized water

was added to the flask to terminate the hydrolysis process. The fresh colloidal suspension of CNCs was filtered with distilled water in a dialysis bag to a constant pH.

2.3. Fabrication of CNCs/alkyl intercalated nanocomposites

CNCs aqueous suspension was solvent exchanged to acetone and then to dichloromethane, and finally to dry toluene by several extraction operations. CNCs/alkyl intercalated nanocomposites were fabricated through the in situ intercalative chemical reaction between terminal groups of N-octadecyl isocyanate molecules and hydroxyl groups on the (200) lattice planes in CNCs (Siqueira et al., 2013). N-Octadecyl isocyanate, 10 equivalents according to the hydroxyl groups available at CNCs was slowly added to the CNCs toluene solution in a three-necked round-bottomed flask equipped with a reflux condenser under nitrogen atmosphere at 90 °C. The temperature was then increased up to 110 °C, and it was kept in this condition for 2 h. The reaction system was washed with ethanol by centrifugation/redispersion at 12000 rpm and 10 °C for 10 min each step for 10 times to remove both amines formed during the reaction and unreacted isocyanates.

2.4. Characterizations

The morphology of CNCs was observed under a TEM (HT7700, Hitachi High Technologies, Japan) and a scanning probe microscope (Multimode Nanoscope IIIa controllor, Veeco Company, USA). The lengths and widths of the CNCs were analyzed with Image J software (National Institutes of Health, USA) and 100 CNCs were randomly selected for the measurements. The thickness of CNCs was analyzed with Nanoscope Analysis software (Bruker Company, German) and more than 30 particles were randomly selected for each measurement. Attenuated total reflection-Fourier transform infrared (FT-IR) spectra of freeze-dried CNCs and dried CNCs/alkyl intercalated nanocomposites were recorded in a FT-IR spectrometer (Magna-IR 750, Nicolet Company, USA) at a resolution of 4 cm^{-1} in the range of 4000 cm^{-1}–400 cm^{-1}. At least two measurements for different samples were performed to check reproducibility. Elemental analysis (vario EL, Elementar Analysensysnteme GebH Company, German) was used to determine the atomic composition (carbon, hydrogen and nitrogen contents) for freeze-dried CNCs and dried CNCs/alkyl intercalated nanocomposites samples. The results from elemental analysis were used to determine the degree of substitution (DS, number of grafted hydroxyl function per anhydroglucose unit (AGU)) according to Eq. (1) (Siqueira et al., 2013):

$$DS = (72.07 - C \times 162.14)/(281.48 \times C - 216.20) \qquad (1)$$

where C is the relative carbon content in the sample and 72.07, 162.14, 281.48 and 216.20 corresponding to the carbon mass of the anhydroglucose unit, mass of anhydroglucose unit, mass of n-octadecyl isocyanate residue and carbon mass of the n-octadecyl isocyanate residue, respectively.

Crystalline structures of freeze-dried CNCs, dried CNCs/alkyl intercalated nanocomposites and n-octadecyl isocyanate were studied on a diffractometer (D8 advance XRD, Bruker Company, Germany), using Cu Kα radiation (λ = 0.154 nm, 40 kV and 40 mV) from 2θ = 3–40° at a scan rate of 4°/min. Differential scanning calorimetry (DSC) was performed on a DSC 200F3 (NETZSCH Company, Germany) using nitrogen as the purge gas. Samples were heated from −20 °C to 570 °C at a rate of 10 °C/min, except for n-octadecyl isocyanate, whose heating range was −30 °C–120 °C. For studying the crystallization of intercalated alkyls in CNC/alkyl intercalated nanocomposites, a heating-cooling cycle measurement was conducted. Dried CNCs/alkyl intercalated nanocomposites were first heated to 170 °C from −20 °C at a heating rate of 10 °C/min
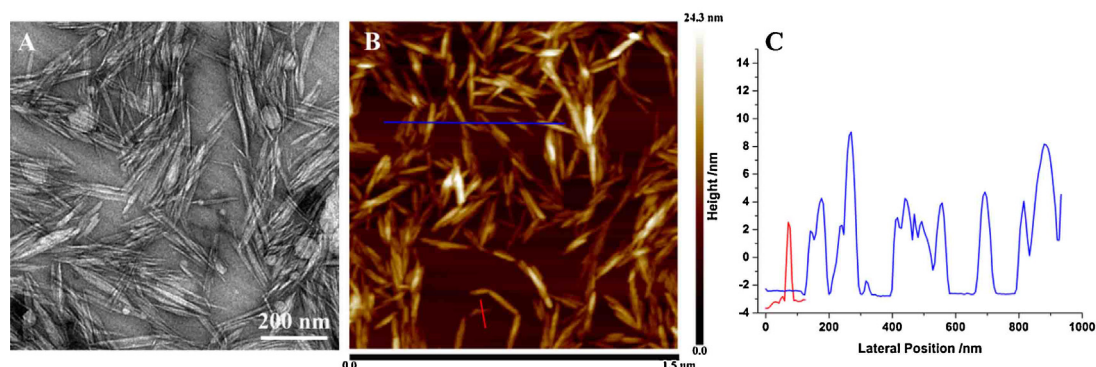
Fig. 1. TEM image A) and AFM image B) of CNCs, respectively. C) Height profiles of the cross sections along the paths are indicated by the red and blue lines in the AFM images. (For interpretation of the references to colour in this figure legend, the reader is referred to the web version of this article.)

and held for 5 min, and then they were cooled to $-20\,^\circ$C at a cooling rate of 2 $^\circ$C/min. After holding at $-20\,^\circ$C for 10 min, they were reheated to 170 $^\circ$C at a rate of 10 $^\circ$C/min. Thermogravimetric analysis was carried out under dry nitrogen purge from 30 $^\circ$C to 650 $^\circ$C at 10 $^\circ$C/min using STA 449F3 (NETZSCH Company, Germany).

3. Results and discussion

CNCs were isolated from filter papers by sulfuric acid hydrolysis during ultrasonic treatment, as in our previous study (Guo, Guo et al., 2016). They have a needle-like morphology with the dimensions of 76.4 ± 17.5 nm, 4.9 ± 0.6 nm and 5.4 ± 0.9 nm for the length, width and thickness of CNCs, respectively (Fig. 1, Fig. 2). CNCs were further used as the intercalation host to fabricate CNCs/alkyl intercalated nanocomposites. The intercalation of *n*-octadecyl isocyanate molecules was realized through the in situ intercalative chemical reaction between the terminal groups of *N*-octadecyl isocyanate molecules and hydroxyl groups in CNCs following the procedure developed by Siqueira et al. (Espino-Pérez et al., 2013; Siqueira, Bras, & Dufresne, 2010; Siqueira et al., 2013) for a long reaction period (2 h).

The resultant CNCs/alkyl intercalated nanocomposites display the strong and typical ester carbonyl stretching band at 1727 cm^{-1}, hydrogen bonded carbonyl stretching band at 1679 cm^{-1}, amide I vibration at 1615 cm^{-1}, amide II vibrations at 1570 cm^{-1}, amide II vibrations at 1534 cm^{-1}, and a strong increase in the band characteristic of the grafted alkyl chain at 2956 cm^{-1} (γ_{as}CH$_3$), 2872 cm^{-1} (γ_sCH$_3$), 2920 cm^{-1} (γ_{as}CH$_2$), and 2849 cm^{-1} (γ_sCH$_3$) (Fig. 2) (Espino-Pérez et al., 2013; Siqueira et al., 2010, 2013). This indicates that CNCs are successfully modified by *n*-octadecyl isocyanate molecules. Meanwhile, the structure of cellulose backbone is maintained after intercalation, which is confirmed by the presence of cellulose characteristic peaks centered at 1163 cm^{-1} (glycosidic link symmetric deformation) and 1108 cm^{-1} (COC ring breathing) in the resultant intercalated nanocomposites (Li &
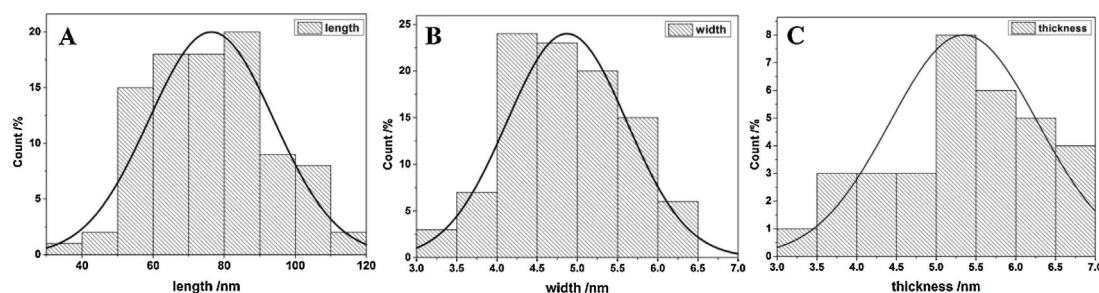
Renneckar, 2011). Besides, the excess of *n*-octadecyl isocyanate has been wholly removed in the CNCs/alkyl intercalated nanocomposites due to the absence of the isocyanate group signal at 2260 cm^{-1} belonged to pure *n*-octadecyl isocyanate.

Elemental analysis was further used to obtain the degree of substitution for the *n*-octadecyl isocyanate in CNCs/alkyl intercalated nanocomposites (Table 1). Using Eq. (1) (Siqueira et al., 2013), the degree of substitution is estimated to around 1.8, meaning that almost two alkyl substituents are introduced into every anhydroglucose unit of cellulose in CNCs/alkyl intercalated nanocomposites. This is also proven by the changes of hydroxyl groups in CNCs using FTIR spectroscopy (Fig. 3). Three kinds of OH vibrations in cellulose I$_\beta$ allomorph are peaked around 3405 cm^{-1}, 3340 cm^{-1} and 3268 cm^{-1} respectively, which are related to hydroxyl groups involved in O(2)H$\cdots$O(6) hydrogen bond, O(3)—H$\cdots$O(5) hydrogen bond, and O(6)—H$\cdots$O(2) hydrogen bond, respectively (Guo, Guo et al., 2016; Li, & Renneckar, 2011). After intercalation, the intensities of peaks at 3268 cm^{-1} and 3405 cm^{-1} for CNCs/alkyl intercalated nanocomposites dramatically reduce. While, the peak at 3340 cm^{-1} still has the strong intensity, in consistent with the presence of peak at 1058 cm^{-1} related to the stretching of the CO in the C$_3$ position involved in the intrachain hydrogen boning O(3)H$\cdots$O(5) bond. These indicate that both O(6)—H and O(2)—H hydroxyl groups instead of O(3)—H within (200) lattice planes in CNCs are mostly reacted with the terminal groups of *n*-octadecyl isocyanate during the in situ intercalative chemical reaction. Therefore, in CNCs/alkyl intercalated nanocomposites, *n*-octadecyl isocyanate molecules are attached to the (200)

Table 1
Elemental analysis results of CNCs and CNCs/alkyl intercalated nanocomposites.

|	C%	H%	N%	S%
CNCs	42.1	6.3	0.0	1.8
CNCs/alkyl intercalated nanocomposites	68.9	14.7	4.3	0.0

Fig. 2. A) Length, B) width and C) thickness distributions of the CNXCs.
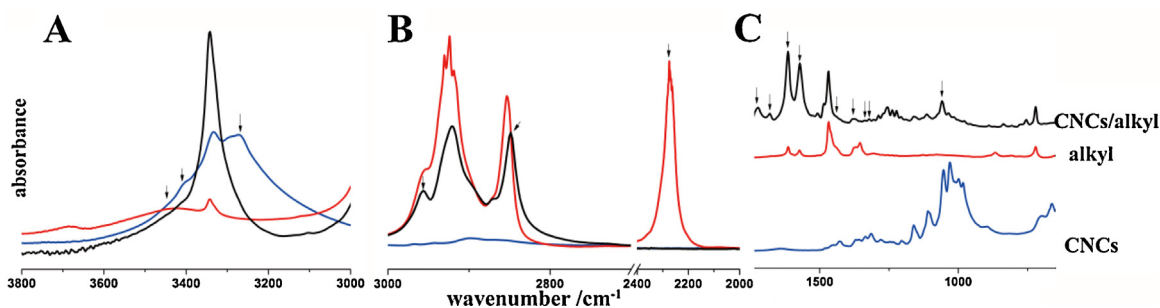
Fig. 3. FTIR spectra of CNCs (the blue line), *n*-octadecyl isocyanate (the red line) and CNCs/alkyl intercalated nanocomposites (the black line). A) 3800–3000 cm^{-1} range; B) 3000–2000 cm^{-1} range; C) 1800–650 cm^{-1} range. (For interpretation of the references to colour in this figure legend, the reader is referred to the web version of this article.)
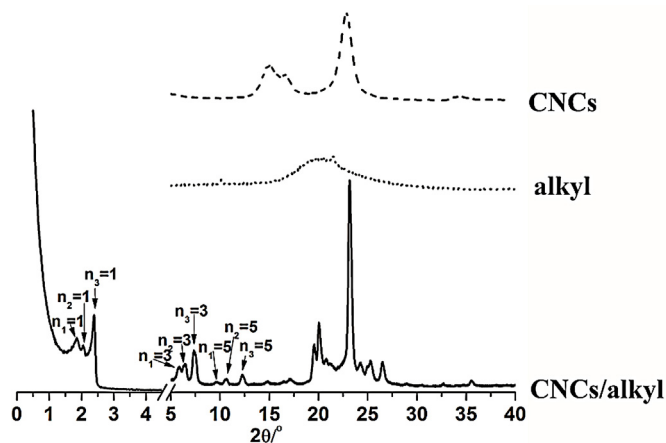
Fig. 4. XRD profiles of CNCs (the dash line), *n*-octadecyl isocyanate (the dot line) and CNCs/alkyl intercalated nanocomposites (the solid line) in the small angle range (2θ < 5°) and wide angle range (5° < 2θ < 40°).

lattice planes in CNCs via the covalent bonds between their terminal groups and hydroxyl groups O(6)—H and O(2)—H in CNCs and form a dense alkyl brushes due to the high degree of substitution.
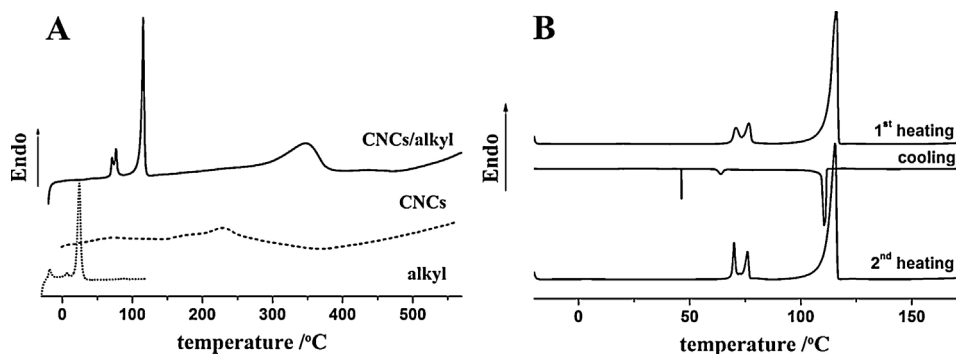
The intercalation structure is clarified by X-ray diffraction. XRD profiles of CNCs (the dash line), *n*-octadecyl isocyanate (the dot line) and CNCs/alkyl intercalated nanocomposites (the solid line) in both the small angle range (2θ < 5°) and the wide angle range (5° < 2θ < 40°) are shown in Fig. 4. CNCs show a characteristic peak of cellulose I$_\beta$ allomorph (d$_{200}$ = 0.39 nm) at 22.8° of 2θ. *N*-Octadecyl isocyanate is in the noncrystalline state at 30 °C due to its melting point around 24 °C calculated by the below DSC curve. After intercalation, significant variations in the d-spacing of (200) lattice plane for CNCs can be detected. In the XRD spectrum of CNCs/alkyl intercalated nanocomposites, several new diffraction peaks at 2θ range of 1.5–13° are present. Results appear to suggest three sets of d-spacings in CNCs/alkyl intercalated nanocomposites, one set with the primary reflection at 47.8 Å (2θ = 1.9°) together with the third order at 15.2 Å (2θ = 5.9°) and the fifth order at 9.1 Å (2θ = 9.6°), the second set with the primary reflection at 43.0 Å (2θ = 2.0°) together with the third order at 13.7 Å (2θ = 6.5°) and the fifth order at 8.3 Å (2θ = 10.6°), and the third set with the primary reflection at 36.9 Å (2θ = 2.4°) together with the third order at 12.0 Å (2θ = 7.4°) and the fifth order at 7.3 Å (2θ = 12.3°). With the thickness of (200) lattice plane in CNCs, calculated as 3.9 Å and the distance of repeating units (2.54 Å) for the trans zigzag chain of alkanes (Matsumoto, Oshita, & Fujioka, 2002), the enlargement of the interlayer spacing in CNCs/alkyl intercalated nanocomposites implies that *n*-octadecyl isocyanate molecules have been intercalated in CNCs successfully and formed the dense hydrocarbon chain brushes on the (200) lattice surfaces in CNCs. The simplest structural rep-

resentation for these basal spacings of 47.8 Å, 43.0 Å and 36.9 Å would involve a bilayer model in which intercalated *n*-octadecyl isocyanate was attached to the cellulose (200) lattice plane, as proposed for alkyl-substituted (hydroxyl propyl) cellulose (Lee, Pearce, & Kwei, 1997b).

Furthermore, the significant lateral crystallization of attached alkyls in CNCs/alkyl intercalated nanocomposites is evident from the narrow diffraction peaks in the region of 2θ = 19–27° (Fig. 4). There are a strong peak at 23.2° (d = 3.8 Å) and other diffraction signals at 19.5° (d = 4.5 Å), 20.0° (d = 4.4 Å), 20.8° (d = 4.3 Å), 21.2° (d = 4.2 Å), 24.3° (d = 3.7 Å) and 25.0° (d = 3.6 Å). Based on the *n*-paraffin crystal structure (Broadhurst, 1962; Lee, Pearce, & Kwei, 1997a; Lee et al., 1997b), it suggests that the intercalated alkyls in CNCs/alkyl intercalated nanocomposites exhibit characteristic reflections of α$_H$ (α-hexagonal phase) (4.2, 2.4, 2.1 Å), β$_H$ (β-triclinic phase) (4.5, 3.8 and 3.6 Å), and β$_O$ (β-triclinic phase) (3.7 Å) crystalline forms of long-chain hydrocarbons, as reported in the previous studies about alkyl substituted comblike semiflexible polymers with side branches exceeding a certain number of methylenic units (Crépy, Miri, Joly, Martin, & Lefebvre, 2011; Lee et al., 1997b; López-Velázquez, Bello, & Pérez, 2004).

The ordered molecular arrangement of intercalated alkyls in CNCs/alkyl intercalated nanocomposites can also be proven by the variation of molecular conformation via FTIR spectroscopy. In general, both frequency and width of γ$_{as}$ (CH$_2$) in the alkyl chains are sensitive to the gauche/trans conformer ratio and the packing density of methylene chains. As the number of gauche conformations along the hydrocarbon chain (chain disorder) increases, the γ$_{as}$ (CH$_2$) band shifts from the lower frequency, characteristic of highly ordered all-trans formation, to the higher frequency and its peak width becomes wider (Vaia, Teukolsky, & Giannelis, 1994). As shown in Fig. 3B, *n*-octadecyl isocyanate has the characteristic peak at 2853 cm^{-1} for γ$_s$(CH$_2$) stretching, and split peaks at 2920 cm^{-1}, 2923 cm^{-1} and 2930 cm^{-1} for γ$_{as}$(CH$_2$) stretching. It indicated that at room temperature pure *n*-octadecyl isocyanate was in a less ordered arrangement due to its low melting point. While, once *n*-octadecyl isocyanate was intercalated into CNCs, it organized in the ordered crystalline state. As shown in Fig. 3B, the spectrum towards CNCs/alkyl intercalated nanocomposites, displays peaks at 2848 cm^{-1} and 2920 cm^{-1} for γ$_s$(CH$_2$) and γ$_{as}$(CH$_2$) stretching, indicating that the intercalated hydrocarbon chains in CNCs/alkyl intercalated nanocomposites are in the all-trans ordered crystalline state (Vaia et al., 1994).

The crystalline state of intercalated *n*-octadecyl isocyanate in CNCs/alkyl intercalated nanocomposites was further studied by DSC (Fig. 6A). CNCs show a broad endothermic peak below 100 °C, followed by a bigger endothermic peak at 230 °C with a shoulder at 183 °C. The former endothermic peak is ascribed to the vaporization of the water contaminant (López-Velázquez et al., 2004; Tan, Hamid, & Lai, 2015), in accordance with the first weight loss below 120 °C in TGA studies (Fig. 6). The peak at 230 °C is attributed

Fig. 5. A) First heating DSC scans of as-made CNCs (the dash line), *n*-octadecyl isocyanate (the dot line) and CNCs/alkyl intercalated nanocomposites (the solid line). B) DSC traces of CNCs/alkyl intercalated nanocomposites at a heating rate of 10 °C/min. First heating scans of the as-made samples (top), cooling after holding at 170 °C for 5 min at a rate of 2 °C/min (middle) and the second heating after holding at −20 °C for 10 min at a rate of 10 °C/min (bottom). Traces have been shifted vertically.

to the melting (or decomposition) of CNCs. After intercalation, CNCs/alkyl intercalated nanocomposites showed a distinct melting region between 65 °C and 130 °C with a maximum at 115 °C and a double peak at 71 °C and 76 °C, followed by the degradation around 349 °C. In comparison with the DSC curve of pure *n*-octadecyl isocyanate, the melting signal of pure *n*-octadecyl isocyanate crystals is absent, which is consistent with FTIR results (Fig. 3).

For CNCs/alkyl intercalated nanocomposites, the observed signals below 150 °C should be attributed to the covalently bonded long chain alkyl crystals, whose melting point is much higher than that of pure *n*-octadecyl isocyanate (Fig. 5A, the dot line). The increase of melting point is the result of the reduction of entropy change during melting, which is consistent with our previous studies (Guo et al., 2011; Guo, Fu et al., 2016). The sharp endotherm at 115 °C (T_1) is belonged to the isotropization of intercalated alkyls in CNCs/alkyl intercalated nanocomposites (Lee et al., 1997a). And the double-melting peak (T_2) at 71 °C and 76 °C is ascribed to the melting points of lateral crystallization of attached alkyl brushes in CNCs/alkyl intercalated nanocomposites, as already observed for similar cellulose derivatives (Crépy et al., 2011; López-Velázquez et al., 2004; Lee et al., 1997a). The double-melting peak at 71 °C and 76 °C is indicative of nonuniform or multiple arrangements of attached long chain alkyl crystal formation, in accordance with the mixture crystalline forms of intercalated alkyls by XRD results (Fig. 4).

Integration of the CNCs melting signals between 120 °C and 320 °C (Fig. 5A) results in a heat of fusion of 229.3 J/g, whereas CNCs/alkyl intercalated nanocomposites upper signals give a value of 243.6 J/g. This indicates that cellulose molecules in CNCs/alkyl intercalated nanocomposites are in the more ordered crystalline state. Besides, integration of the alkyl melting signals in CNCs/alkyl intercalated nanocomposites results in a heat of fusion of 189.3 J/g, whereas pure *n*-octadecyl isocyanate upper signals give a value of 105.4 J/g (Fig. 5A, the dot line). It showed that the intercalation promoted the arrangement of alkyls. Intercalated alkyls were in the more ordered crystalline state, in agreement with the all-trans ordered crystalline state illustrated by FTIR results (Fig. 3).

In order to gain insight of above transitions towards intercalated alkyls in CNCs/alkyl intercalated nanocomposites, a heating-cooling cycle was performed (Fig. 5B). The isotropizations of intercalated alkyls (T_1) and their lateral crystallization melting (T_2) respond similarly towards the heating scan and the cooling scan. Besides, the locations of T_1 and T_2 remain the same in the second heating scan. The thermogram recorded for CNCs/alkyl intercalated nanocomposites during the slow cooling scan after holding at 170 °C for 5 min shows the crystallization exotherm located at 111 °C (T_1), and two separated peaks at 46 °C and 64 °C (T_2). It means
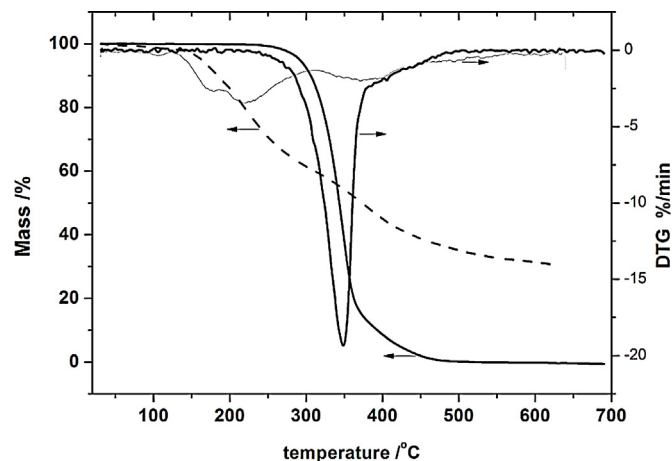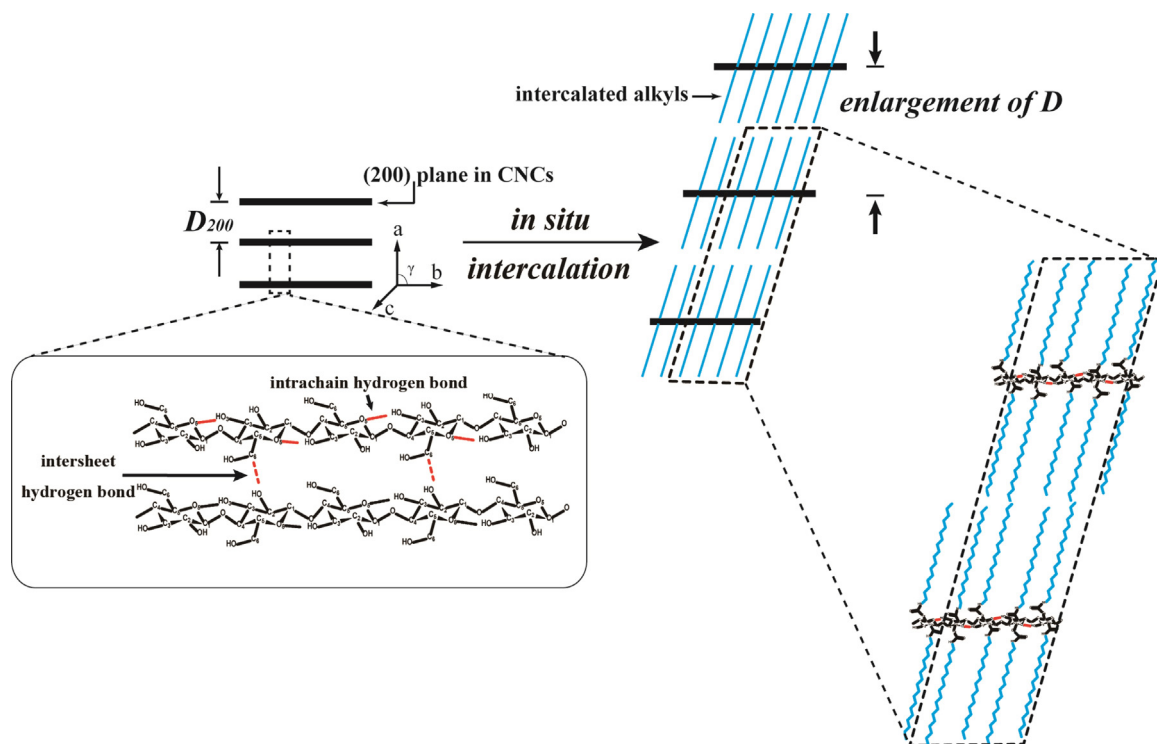
the kinetics of crystallization of intercalated alkyls in CNCs/alkyl intercalated nanocomposites is fast.

CNCs/alkyl intercalated nanocomposites also display a significant increase of decomposition temperature for CNCs from 230 °C (Fig. 5A, the dash line) to 349 °C (Fig. 5A, the solid line), which is similar to the melting temperature of microcrystalline cellulose (Tan et al., 2015). It is probably resulted from both the more ordered crystalline structure formed during intercalation or/and the removal of hydrogen sulfate anion on the surface of CNCs during chemical modification at 110 °C for 2 h, as indicated by the elemental analysis (Table 1).

The pyrolysis property of CNCs/alkyl intercalated nanocomposites is further studied. Thermogravimetric (TG) and its derivatives (DTG) curves of CNCs and CNCs/alkyl intercalated nanocomposites are shown in Fig. 6. CNCs display the first weight loss below 120 °C corresponding to the evaporation of absorbing water. Then, a fast weight loss is observed until 218 °C, and the third-step thermal degradation reaction at 370 °C, after which the degradation continues until a full decomposition at around 560 °C with a mass yield of char produced by CNCs, 31% (Fig. 6, the dash line). The first pyrolysis occurred at a lower temperature (220 °C) is belonged to the decomposition of highly accessible and sulfated amorphous regions while the second pyrolysis which took place at higher temperature (370 °C) is ascribed to the breakdown of the unsulfated part of the crystal interior (Tan et al., 2015). After the intercalation of these dense crystalline long alkyl brushes on the (200) lattice planes in CNCs, no weight loss below 100 °C attributable to the removal of absorbed water is observed

Fig. 6. TGA curves (left) and DTG curves (right) of CNCs (the dash line) and CNCs/alkyl intercalated nanocomposites (the solid line).

Scheme 1. Schematic drawing of intercalation structure model for CNCs after the in situ intercalation, cross section view (chain direction perpendicular to paper plane).

for CNCs/alkyl intercalated nanocomposites, due to the hydrophobic modification of CNCs using *n*-octadecyl isocyanate. Similar absence of water uptake and consequent elimination in TGA has been observed before with hydrocarbon chain-modified celluloses (Rosilo, Kontturi, Seitsonen, Kolehmainen, & Ikkala, 2013). Moreover, the major degradation step is shifted to the higher temperature and begins at 250 °C. However, a greater weight loss than CNCs is observed beyond this point until a full decomposition at around 480 °C. It might be resulted from the ordered crystalline structure in CNCs/alkyl intercalated nanocomposites. Besides, the absence of sulfuric content in CNCs/alkyl intercalated nanocomposites also contributes. Sulfuric groups on the CNCs surface are known to considerably decrease the onset temperature of thermal degradation due to desulfation and subsequent catalysis of decomposition reactions by the released sulfuric acid. On the other hand, the dehydration effect catalyzed by the sulfate group would facilitate the formation of char residue (Li & Dufresne, 2014). Therefore, CNCs/alkyl intercalated nanocomposites might have a potential application in the melt extrusion of CNCs reinforced hydrophobic polymers due to their enhanced thermal properties and improved interface compatibility with some hydrophobic matrixes.

On the basis of the presented experimental data, CNCs display their potential as an intercalated host candidate. Through the in situ intercalative chemical reaction, long alkyls were intercalated in CNCs and formed a dense crystalline brushes on (200) lattice planes in CNCs. Besides, intercalated alkyls were fully extended in the all-trans configuration and crystallized in a co-existing organizations of α_H, β_H and β_O crystalline forms in CNCs/alkyl intercalated nanocomposites. These imply that intercalated alkyls would arise from the parallel arrangement instead of the interdigitation. Based on the significant enlargement of interlayer spacing with three sets of d spacings with the primary reflection at 47.8 Å, 43.0 Å and 36.9 Å respectively, and the high degree of substitution of *n*-octadecyl isocyanate at O(6)H and O(2)H hydroxyl groups in CNCs, a simple bilayer model in which intercalated alkyls were attached through covalent bonds between the terminal groups of *N*-octadecyl iso-

cyanate and hydroxyl groups on the (200) lattice planes in CNCs and titled to cellulose (200) lattice plane is proposed (Scheme 1). Furthermore, CNCs/alkyl intercalated nanocomposites possessed increased thermal properties and decreased char residue.

4. Conclusions

CNCs are an intercalated host candidate, due to their layered structure and the weak intersheet interactions. In this paper, CNCs/alkyl intercalated nanocomposites were fabricated through the in situ intercalative chemical reaction between the terminal groups of *N*-octadecyl isocyanate molecules and hydroxyl groups on the (200) lattice planes in CNCs. The intercalation of alkyls resulted in a significant enlargement of interlayer spacing, compared with the d-spacing of CNCs (0.39 nm). Moreover, intercalated alkyls were fully extended in the all-trans configuration and crystallized in a co-existing organization of α_H, β_H and β_O crystalline forms. Considering intercalated alkyls in a high degree of substitution at O(6)H and O(2)H hydroxyl groups in CNCs and their ordered packing, the molecular arrangement in the resultant intercalated nanocomposites would involve a bilayer model in which intercalated alkyls were ordered packing and titled to cellulose (200) lattice plane. Besides, the resultant intercalated nanocomposites displayed the increased thermal properties and decreased char residue.

References

Berman, A., Hanson, J., Leiserowitz, L., Koetzle, T. F., Weiner, S., & Addadi, L. (1993). Biological control of crytssal texture: A widespread strategy for adapting crystal properties to function. *Science, 259*, 776–779.

Biradha, K., Dennis, D., MacKinnon, V. A., Sharma, C. V. K., & Zaworotko, M. J. (1998). Supramolecular synthesis of organic laminates with affinity for aromatic guests: A new class of clay mimics. *Journal of the American Chemical Society, 120*, 11894–11903.

Bott, S. G., Coleman, A. W., & Atwood, J. L. (1988). Intercalation of cationic, anionic, and molecular species by organic hosts. Preparation and crystal structure of $[NH_4]_6[calix[4]areanesulfonate]$ $[MeOSO_3]$.cntdot.$(H_2O)_2$. *Journal of the American Chemical Society, 110*, 610–611.

Broadhurst, M. G. (1962). An analysis of the solid phase behavior of the normal paraffins. *Journal of Research of the National Bureau of Standards, 66A*, 241–249.

Crépy, L., Miri, V., Joly, N., Martin, P., & Lefebvre, J. (2011). Effect of side chain length on structure and thermomechanical properties of fully substituted cellulose fatty esters. *Carbohydrate Polymers, 83*, 1812–1820.

Deng, H., Lin, P., Xin, S., Huang, R., Li, W., Du, Y., et al. (2012). Quaternized chitosan-layered silicate intercalated composites based nanofibrous mats and their antibacterial activity. *Carbohydrate Polymers, 89*, 307–313.

Espino-Pérez, E., Bras, J., Ducruet, V., Guinault, A., Dufresne, A., & Domenek, S. (2013). Influence of chemical surface modification of cellulose nanowhiskers on thermal, mechanical, and barrier properties of poly(lactide) based bionanocomposites. *European Polymer Journal, 49*, 3144–3154.

Giovanella, U., Leone, G., Galeotti, F., Mróz, W., Meinardi, F., & Botta, C. (2014). FRET-assisted deep-blue electroluminescence in intercalated polymer hybrids. *Chemistry of Materials, 26*, 4572–4578.

Guo, J., Zhu, L., Jiang, M., & Chen, D. (2011). Deliberately designed processes to physically tether the carboxyl groups of poly(pentacosadiynoic acid) to a poly(vinyl alcohol) glassy matrix to make poly(pentacosadiynoic acid) thermochromically reversible in the matrix. *Langmuir, 27*, 6651–6660.

Guo, J., Fu, K., Zhang, Z., Yang, L., Huang, Y., Huang, C., et al. (2016). Reversible thermochromism via hydrogen-bonded cocrystals of polydiacetylene and melamine. *Polymer*, http://dx.doi.org/10.1016/j.polymer.2016.07.035

Guo, J., Guo, X., Wang, S., & Yin, Y. (2016). Effects of ultrasonic treatment during acid hydrolysis on the yield, particle size and structure of cellulose nanocrystals. *Carbohydrate Polymers, 135*, 248–255.

Habibi, Y., Luci, L. A., & Rojas, O. J. (2010). Cellulose nanocrystals: Chemistry, self-assembly, and applications. *Chemistry Review, 110*, 3479–3500.

López-Velázquez, D., Bello, A., & Pérez, E. (2004). Preparation and characterization of hydrophobically modified hydroxypropylcellulose: Side-chain crystallization. *Macromolecular Chemistry and Physics, 205*, 1886–1892.

Lee, J. L., Pearce, E. M., & Kwei, T. K. (1997a). Side-chain crystallization in alkyl-substituted semiflexible polymers. *Macromolecules, 30*, 6877–6883.

Lee, J. L., Pearce, E. M., & Kwei, T. K. (1997b). Morphological development in alkyl-substituted semiflexible polymers. *Macromolecules, 30*, 8233–8244.

Li, N., & Dufresne, A. (2014). Surface chemistry, morphological analysis and properties of cellulose nanocrystals with gradiented sulfation degrees. *Nanoscale, 6*, 5384–5393.

Li, Q., & Renneckar, S. (2011). Supramolecular structure characterization of molecularly thin cellulose I nanoparticles. *Biomacromolecules, 12*, 650–659.

Lu, Q., Cai, Z., Lin, F., Tang, L., Wang, S., & Huang, B. (2016). Extraction of cellulose nanocrystals with a high yield of 88% by simultaneous mechanochemical activation and phosphotungstic acid hydrolysis. *ACS Sustainable Chemistry & Engineering, 4*, 2166–2172.

Ma, L., Zhang, Y., Meng, Y., & Wang, S. (2015). Preparing cellulose nanocrystals/acrylonitrile-butadiene-styrene nanocomposites using the master-batch method. *Carbohydrate Polymers, 125*, 352–359.

Majoinen, J., Hassinen, J., Haataja, J. S., Rekola, H. T., Kontturi, E., Kostiainen, M. A., et al. (2016). Chiral plasmonics using twisting along cellulose nanocrystals as a template for gold nanoparticles. *Advanced Materials, 28*, 5262–5267.

Matsumoto, A., Odani, T., Sada, K., Miyata, M., & Tashiro, K. (2000). Intercalation of alkylamines into an organic polymer crystals. *Nature, 405*, 328–330.

Matsumoto, A., Oshita, S., & Fujioka, D. (2002). A novel organic intercalation system with layered polymer crystals as the host compounds derived from 1,3-diene carboxylic acids. *Journal of the American Chemical Society, 124*, 13749–13756.

Miyata, M., Shibakami, M., Chirachanchai, S., Takemoto, K., Kasai, N., & Miki, K. (1990). Guest-responsive structural changes in cholic acid intercalation crystals. *Nature, 343*, 446–447.

Moon, R. J., Martin, A., Nairn, J., Simonsen, J., & Youngblood, J. (2011). Cellulose nanomaterials review: Structure, properties and nanocomposites. *Chemical Society Reviews, 40*, 3941–3994.

Oshima, T., Lu, D., Ishitani, O., & Maeda, K. (2015). Intercalation of highly dispersed metal nanoclusters into a layered metal oxide for photocatalytic overall water splitting. *Angewandte Chemie International Edition, 54*, 2698–2702.

Oshita, S., & Matsumoto, A. (2006). Fluorescence from aromatic compounds isolated in the solid state by double intercalation using layered polymer crystals as the host solid. *Langmuir, 22*, 1943–1945.

Rädler, J. O., Koltover, I., Salditt, T., & Safinya, C. R. (1997). Structure of DNA-cationic liposome complexes: DNA intercalation in multilamellar membranes in distinct interhelical packing regimes. *Science, 275*, 810–814.

Ray, S. S., & Okamoto, M. (2003). Polymer/layered silicate nanocomposites: A review from preparation to processing. *Progress in Polymer Science, 28*, 1539–1641.

Rosilo, H., Kontturi, E., Seitsonen, J., Kolehmainen, E., & Ikkala, O. (2013). Transition to reinforced state by percolating domains of intercalated brush-modified cellulose nanocrystals and poly(butadiene) in cross-linked composites based on thiol-ene click chemistry. *Biomacromolecules, 14*, 1547–1554.

Roth, W. J., Gil, B., Makowski, W., Marszalek, B., & Eliášová, P. (2016). Layer like porous materials with hierarchical structure. *Chemical Society Reviews, 45*, 3400–3438.

Siqueira, G., Bras, J., & Dufresne, A. (2010). New process of chemical grafting of cellulose nanoparticles with a long chain isocyanate. *Langmuir, 26*, 402–411.

Siqueira, G., Bras, J., Follain, N., Belbekhouche, S., Marais, S., & Dufresne, A. (2013). Thermal and mechanical properties of bio-nanocomposites reinforced by Luffa cylindrical cellulose nanocrystals. *Carbohydrate Polymers, 91*, 711–717.

Tan, X., Hamid, S. B. A., & Lai, C. W. (2015). Preparation of high crystallinity cellulose nanocrystals (CNCs) by ionic liquid solvolysis. *Biomass and Bioenergy, 81*, 584–591.

Vaia, R. A., Teukolsky, R. K., & Giannelis, E. P. (1994). Interlayer structure and molecular environment of alkylammonium layered silicates. *Chemistry of Materials, 6*, 1017–1022.

Wang, P., Hamad, W. Y., & MacLachlan, M. J. (2016). Structure and transformation of tactoids in cellulose nanocrystal suspensions. *Nature Communications, 7*, 11515.

Whittingham, M. S. (1982). Intercalation chemistry. In M. S. Whittingham, & A. J. Jacobson (Eds.),. London: Academic Press.

Zhang, X., Hou, Z., Li, X., Liang, J., Zhu, Y., & Qian, Y. (2016). MoO_2 nanoparticles as high capacity intercalation anode material for long-cycle lithium ion battery. *Electrochimica Acta, 213*, 416–422.

Zhang, X., Sun, P., Liu, H., Shang, S., Song, J., & Wang, D. (2016). Extraction and comparison of carboxylated cellulose nanocrystals from bleached sugarcane bagasse pulp using two different oxidation methods. *Carboxylate Polymers, 138*, 237–243.